NACA

RESEARCH MEMORANDUM

NOTE ON SOME OBSERVED EFFECTS OF ROCKET-MOTOR OPERATION ON THE BASE PRESSURES OF BODIES IN FREE FLIGHT

By Paul E. Purser, Joseph G. Thibodaux, and H. Herbert Jackson

Langley Aeronautical Laboratory
Langley Air Force Base, Va.

NATIONAL ADVISORY COMMITTEE FOR AERONAUTICS

WASHINGTON

November 16, 1950

Classification cancelled (or changed to UNCLASSIFIED)

By Authority of NASA TECH PUB ANNOUNCEMENT #107
(OFFICER AUTHORIZED TO CHANGE)

By 9604756
NAME AND

.....
GRADE OF OFFICER MAKING CHANGE)

4 Sept 61
DATE

NACA RM L50I18

NATIONAL ADVISORY COMMITTEE FOR AERONAUTICS

RESEARCH MEMORANDUM

NOTE ON SOME OBSERVED EFFECTS OF ROCKET-MOTOR OPERATION ON THE BASE PRESSURES OF BODIES IN FREE FLIGHT

By Paul E. Purser, Joseph G. Thibodaux,
and H. Herbert Jackson

SUMMARY

Some measurements of the effects of rocket-motor operation on base pressure were obtained incidental to other research on some bodies in free flight. These data are presented and qualitatively analyzed. The analysis indicates that jet effects on drag are of sufficient importance to deserve consideration in the design of jet-motor nozzles, especially for aircraft and missiles where the thrust and drag are of the same order of magnitude. Since the data were obtained incidentally during research for other purposes, they are not systematic enough for general design use. The data indicate, however, that a large, wide-angle underexpanded jet (jet-exit pressure greater than atmospheric) will cause a decrease in the suction that exists on the base annulus around the jet exit, whereas an overexpanded jet may increase the suction on the annulus. The data also indicate that increasing the nozzle divergence angle or the nozzle size relative to the base will tend to decrease the base suction. The base-pressure changes induced by the jet should be considered in the structural design of the outer body skin on the rear part of fuselages containing jets.

INTRODUCTION

The use of jet and rocket motors has resulted in an interest in the effects of the operation of such power plants on the external drag of the bodies in which they are housed. These power effects on drag may be roughly divided into two parts: one, the aspirating and blocking effects of the jet which might modify the boundary layer and thus the friction and pressure drag on the sides of the body; and the other, the effects of the jet on the pressure or suction that exists on the annulus at the base

of the body between the jet nozzle and the body edge. References 1 and 2 present some data on the effects of jets on body side pressure and drag. Few data, however, are available on the effects of jets on body base pressure.

Some power effects on base pressure have been noted in measurements obtained on rocket-powered models flown for other purposes; for example, such data were obtained in the investigations reported in references 3 and 4. In order to obtain some preliminary insight into the jet effects on base pressure, both the "power-on" and "power-off" portions of these pressure records were evaluated. Some of these data are presented and discussed herein. The discussion deals with the observed jet effects on base pressure, with the effects on rocket-motor thrust of changes in nozzle design which are shown to affect the base pressure, and with structural aspects of jet-induced changes in base pressure.

SYMBOLS

Some of the symbols and terms used in the following pages are defined graphically in figure 1.

M	Mach number, V/c
p	atmospheric static pressure, pounds per square inch, absolute
p_b	pressure measured in model base chamber between rocket nozzle and model skin, pounds per square inch, absolute
p_j	estimated rocket-nozzle exit static pressure, pounds per square inch, absolute
p_c	rocket-chamber pressure, pounds per square inch, absolute
V	velocity of model
c	velocity of sound
q	dynamic pressure
γ	specific heat ratio
α	nozzle-divergence half angle, degrees
A_e	rocket-nozzle exit area, square inches

A_t rocket-nozzle throat area, square inches

D_b outside diameter of model base, inches

D_j diameter of rocket-nozzle exit, inches

D diameter

X longitudinal distance from fuselage nose to station on body

L length of body

F thrust of rocket motor, pounds

C_N thrust coefficient $\left(\frac{F}{\lambda A_t p_c}\right)$

λ nozzle-divergence correction to thrust

ε expansion ratio (A_e/A_t)

MODELS AND FLIGHT TESTS

The models for which data are herein presented were fin-stabilized bodies of revolution. The coordinates for the bodies are given in table I. The external shapes of the models are shown in figure 2 and details of the base configurations are shown in figure 3. The propulsion units used for each model are shown in table II.

The pertinent design variables covered by the present models are: (1) jet-exit pressure, (2) nozzle expansion angle, and (3) ratio of model base diameter to nozzle-exit diameter.

The models were flown at the Langley Pilotless Aircraft Research Station, Wallops Island, Va. All models were launched at elevation angles varying from 60° to 75°, thus their flight paths during powered flight and during the high Mach number ($M > 0.8$) gliding flight were very nearly straight lines.

The velocity in each case was measured by means of a CW Doppler radar "velocimeter." Atmospheric data necessary for converting velocity to Mach number and to provide static pressures were obtained from the NACA modified SCR-584 radar tracking unit and by radiosondes released at the time of firing.

[redacted]

The pressures existing in the annular chamber at the base of the model were measured and transmitted to the ground by means of standard NACA telemeter instrumentation.

The "power-on" values of p_b presented in a subsequent section of this paper are those measured during the sustainer-powered portion of the flight. The "power-off" values of p_b are those measured during gliding flight corrected by use of the following equation to the atmospheric conditions prevailing during powered flight at the same Mach number for the same model.

$$p_b(\text{power-off}) = \frac{p_b - p}{q}(\text{gliding flight})Xq(\text{powered flight}) + p(\text{powered flight})$$

DETERMINATION OF JET-EXIT PRESSURE

Values of jet-exit pressure were required for analyzing and discussing the observed effects of jet operation on base pressure. Since no values of jet-exit pressure were measured in these tests, it was necessary to calculate values of p_j from chamber-pressure-time histories that were estimated for each flight test. Experience over a number of years of static and flight testing shows that for all supposedly identical rockets that are produced under carefully controlled conditions, the chamber-pressure-time histories of rocket firings are reproducible and are a function of initial powder temperature only. The burning time of each motor was obtained from telemetered data, and the chamber-pressure-time history for the rocket motor used in flight was fitted to the burning time. The thermodynamic properties of the exhaust gases were obtained from a knowledge of the propellant composition for each rocket used. The nozzle geometry for each rocket was known and the jet pressures were calculated from the following relationship which also appears in reference 5:

$$\frac{A_e}{A_t} = \frac{\left(\frac{2}{\gamma+1}\right)^{\frac{\gamma+1}{2(\gamma-1)}}}{\left(\frac{p_j}{p_c}\right)^{\frac{1}{\gamma}}\sqrt{\frac{2}{\gamma-1}\left[1-\left(\frac{p_j}{p_c}\right)^{\frac{\gamma-1}{\gamma}}\right]}}$$

Since the area ratio A_e/A_t and the ratio of specific heats do not change for a specific rocket, the exit pressure is a function of chamber pressure only:

$$p_j = f(p_c)$$

This relationship is not valid when the exhaust gases do not continue to fill the nozzle, that is, when jet separation takes place.

Investigations reported in references 5 to 7 indicate that in static tests the jet pressure at which separation occurs is primarily dependent on atmospheric pressure and chamber pressure and is relatively independent of propellant composition, gas temperature, specific heat ratio, total expansion ratio, and nozzle divergence angle. These static tests show that separation in the nozzle occurs when the jet-exit pressure approaches 40 percent of atmospheric pressure although the separation pressure decreases slightly with increases in chamber pressure. In free flight separation probably occurred at a pressure between 40 percent of atmospheric pressure and 40 percent of power-on base pressure. As a conservative procedure, however, it was assumed for the present analysis that isentropic overexpansion in the nozzle was possible down to pressures of 0.4 atmospheric pressure.

RESULTS AND DISCUSSION

Observed Pressures

The pertinent data are presented in figures 4 to 7 as plots of pressure and Mach number against time measured from the instant of firing of the sustainer or internal rocket. It should be noted that the values of p_b(power-off) presented were not measured at the times shown, but, as previously stated, are values measured during gliding flight corrected to the atmospheric conditions existing during powered flight at the same Mach number.

It can be seen from figures 4 to 7 that operation of the rockets had a marked effect on the model base pressure. For models A and B, during the time at which the rocket jets were underexpanded (exit pressure greater than atmospheric) the model base pressures were increased from the power-off value, whereas during the time at which the rocket jets were overexpanded the model base pressures tended to decrease. For models C and D the effects were opposite to those for models A and B, that is, the underexpanded jet generally decreased the base pressures from the power-off values. In order to discover whether some pattern existed in the effects noted, the data were summarized and are

presented in figure 8 in the form of ratios of jet pressure and of power-induced change in base pressure to atmospheric static pressure (fig. 8(a)) and to power-off base pressure (fig. 8(b)). Because of the previously noted uncertainty in estimating the pressures to which the jet may expand without separating, only the portions of data pertaining to underexpanded jets are shown. The power-off base pressure was chosen as the reference for use in figure 8 in order to eliminate, at least approximately, the effects on base pressure of such variables as fins and detail shape of the body ahead of the base. Both figure 8(a) and figure 8(b) indicate that in general the direction and magnitude of change in base pressure caused by the jet depend on the jet pressure, the nozzle divergence angle, and, to some extent, on the ratio of base diameter to nozzle-exit diameter. A comparison of the data for models A-3 and B indicates that increasing jet pressure increases the change in base pressure. Comparing the data for models A-1, 2, and 3 indicates that increasing the nozzle divergence angle increases the base pressure. Comparing the data for models A-1, A-2, C, and D indicates that decreases in the ratio of base diameter to nozzle-exit diameter also tend to make the base pressure more positive.

A qualitative explanation of these effects is shown in figure 9. One primary effect of a jet is, through viscous forces and turbulent mixing at the jet boundary, to entrain air and provide an aspirating effect. This aspiration would tend to draw more air around and thus increase the expansion around corner A, figure 9(a). This increased expansion would reduce the base pressure. As indicated by the study reported in reference 8 increases in jet momentum or thrust loading should tend to increase the aspirating effect and thus reduce the base pressure. The jet might also tend to act as a solid body and provide blocking effects similar to those noted for support stings in wind-tunnel tests reported in reference 9. In addition to the viscous and blocking effects the jet would also affect the base pressure through inertia forces. For an underexpanded jet, figure 9(b), the expansion of the jet at the nozzle exit, corner B, would provide inertia forces tending to move the streamline turning around corner A outward, reduce its expansion, and thus increase the base pressure. Decreases in the ratio of base diameter to jet diameter, increases in nozzle divergence angle, and increases in jet pressure (which would increase the turning around corner B) would all tend to make the inertia effects, figure 9(b), overshadow the viscous effects, figure 9(a). Increases in the jet pressure also would mean higher thrust loading for a given rocket motor; this increase in momentum, it is believed, would tend to increase the inertia forces and increase the base pressure which is opposite to the effect of increased thrust loading previously stated for the viscous forces. For an overexpanded jet the flow would shock at corner B, the jet would contract rather than expand, and the inertia forces would tend to be reduced. Although the inertia forces would be less for the

overexpanded jet, increases in jet pressure, nozzle divergence angle, or jet size would still tend, as for the underexpanded jet, to increase the base pressure.

Nozzle Design Procedures

Determination of rocket performance required for any specific missile or airplane is a complex procedure. In general practice, this procedure is carried out neglecting any effects the rocket jet may have on the aerodynamic characteristics of the airplane or missile. Herein, it is assumed that the required motor performance and chamber pressure have been established and the propellant combination has been chosen. Since the jet characteristics are determined by the nozzle design, the effects of nozzle design parameters on thrust are discussed.

The thrust produced by a rocket is given by the following equation:

$$F = \lambda C_N A_t p_c$$

The value λ is a nozzle divergence correction which accounts for the loss in thrust that results from a radial velocity component that exists because the whole jet is not parallel to the thrust axis, and is given by:

$$\lambda = 1/2(1 + \cos \alpha)$$

Values of λ as a function of nozzle divergence half angle α are given in figure 10.

Ease of fabrication usually requires that the supersonic effuser section of the nozzle be a conical shape despite divergence losses. In order to keep nozzle weight to some practical value, nozzle divergence half angles are usually larger than 9°. For any specific motor-missile combination, optimum motor performance, excluding all other effects, may be determined by an analysis of thrust and nozzle weight as a function of nozzle half angle. Nozzle divergence half angles are limited to about 38° as jet separation occurs even in underexpanded nozzles at angles larger than this.

[redacted]

The value C_N, the thrust coefficient, was computed from the following equation which appears in reference 5:

$$C_N = \sqrt{\left(\frac{2\gamma^2}{\gamma - 1}\right)\left(\frac{2}{\gamma + 1}\right)^{\frac{\gamma+1}{\gamma-1}}\left[1 - \left(\frac{p_j}{p_c}\right)\right]^{\frac{\gamma-1}{\gamma}}} + \left(\frac{p_j - p}{p_c}\right)\frac{A_e}{A_t}$$

Values of thrust coefficient as a function of area ratio $\left(\frac{A_e}{A_t}\right)$ and pressure ratio $\frac{p_c}{p}$ are shown in figure 11 for values of γ of 1.2 and 1.3. Values of γ for the exhaust gases of the rockets used were 1.219 and 1.26 as shown in table II.

The total impulse delivered by a rocket is determined by the average thrust coefficient. Since thrust coefficient is a function of free-stream static pressure which may vary along the flight path, optimum total impulse may be determined by an analysis of the average thrust coefficient as a function of area ratio and of the variation in free-stream static pressure along the flight path. In general, for long-range missiles with high launching angles, 60° to 90°, this results in a nozzle that is overexpanded for sea-level conditions and underexpanded at high altitudes.

The previously noted effects of the nozzle design variables on base pressure (or base drag) may be summarized as follows: Base drag probably will be decreased by increases in nozzle divergence angle, jet pressure, and jet size. As an example of the consideration of the effects of nozzle design on both thrust and drag, a brief analysis was made of the effect of varying only the nozzle divergence angle.

The data used were those for models A-1 or A-2 and A-3, figure 8. The increase in nozzle divergence half angle by a factor of three increased the thrusting change in base pressure considerably during the time that the jet was underexpanded. Since both models had the same throat area, chamber pressure, expansion ratio (A_e/A_t), and therefore the same pressure ratio (p_c/p_j), they would both have the same thrust coefficient and all the variables in the equation for thrust would be equal except for λ, the nozzle divergence correction. The fact that models A-1 or A-2 and A-3 had nozzle divergence half angles of 9° and 30°, respectively, meant a net thrust lower for model A-3 by 6 percent or about 102 pounds. The thrusting increment in the pressures on the

base annulus for models A-1 or A-2 and A-3, respectively, are about 1.7 and 6.7 pounds per square inch, absolute (6.5 and 25.9 pounds thrust) and thus are much smaller than 6 percent of the net thrust. Thus, for this case a loss in effective thrust resulted from increasing the nozzle divergence half angle. This, however, may not always be the case. For models in which the total drag is nearly equal to the thrust the pressure drag or thrusting pressures on the base will be an appreciable percentage of the net thrust, perhaps making it possible to increase the effective thrust with an increase in divergence angle. Here again it should be brought to the reader's attention that the power effects only on base pressures are discussed herein and that there are other effects of the jet such as those shown in references 1 and 2 on the side-pressure drag.

Effect of Base Pressure on Structures

In some cases the outer skin at the rear of bodies containing jet motors must be designed on the basis of the pressures existing in the chamber between the jet nozzle and the outer skin. If these pressures are assumed equal to the power-off values of base pressure, they may be in error. For instance, if one assumes that the fuselage side pressure is atmospheric, figure 4(a) indicates collapsing pressures over the rear fuselage skin of 3, 6, or 9 pounds per square inch, depending on whether the design condition chosen is the underexpanded jet, no jet (power-off), or the overexpanded jet.

CONCLUDING REMARKS

Heretofore the aerodynamic design of jet-powered missiles and aircraft has been considered independently of the variables involved within the jet nozzle and the base of the bodies. However, the data herein indicate that these variables should not be neglected.

The effects of a jet on the drag of a missile or aircraft are dependent on the nozzle shape, jet pressure, and ratio of base area to jet-exit area. In the design of rocket nozzles the effects of such rocket design parameters as pressure ratios, area ratios, nozzle divergence angles, and atmospheric conditions along the flight path of the missile on both thrust and external drag should be considered. It is particularly important that the power effects of the jet on body drag be considered in the design of aircraft and missiles where the thrust and drag are of the same order of magnitude. For these cases, small changes in base drag and thrust could have appreciable effects on range and over-all performance.

[redacted]

In the structural design of the fuselage skin in areas vented to the base annulus it is indicated that both power-on and power-off base pressures should be considered because of the relatively great possible differences in these pressures.

Langley Aeronautical Laboratory
National Advisory Committee for Aeronautics
Langley Air Force Base, Va.

[redacted]

REFERENCES

1. Stoney, William E., Jr., and Katz, Ellis: Pressure Measurements on a Sharply Converging Fuselage Afterbody with Jet On and Off at Mach Numbers from 0.8 to 1.6. NACA RM L50F06, 1950.

2. Love, Eugene S.: Aerodynamic Investigation of a Parabolic Body of Revolution at Mach Number of 1.92 and Some Effects of an Annular Jet Exhausting from the Base. NACA RM L9K09, 1950.

3. Jackson, H. Herbert, Rumsey, Charles B., and Chauvin, Leo T.: Flight Measurements of Drag and Base Pressure of a Fin-Stabilized Parabolic Body of Revolution (NACA RM-10) at Different Reynolds Numbers and at Mach Numbers from 0.9 to 3.3. NACA RM L50G24, 1950.

4. Pepper, William B., and Hoffman, Sherwood: Transonic Flight Tests to Compare the Zero-Lift Drag of Underslung and Symmetrical Nacelles Varied Chordwise at the 40-Percent Semispan of 45° Swept-back, Tapered Wing. NACA RM L50G17a, 1950.

5. Garratt, E. P., and Hallett, N. C.: Study of Rockets. Rep. No. E-46-1, Curtiss-Wright Corp., Airplane Div., Nov. 27, 1946.

6. Foster, Charles R., and Cowles, Frederick B.: Experimental Study of Gas-Flow Separation in Overexpanded Exhaust Nozzles for Rocket Motors. Progress Rep. No. 4-103, Jet Propulsion Lab., C.I.T., May 9, 1949.

7. Johnson, Donald F.: Effect of Jet Overexpansion and Separation on Performance of a Rocket Thrust Chamber. Rep. No. 399, Aerojet Engineering Corp., Sept. 13, 1949.

8. Ribner, Herbert S.: Field of Flow About a Jet and Effect of Jets on Stability of Jet-Propelled Airplanes. NACA ACR L6C13, 1946.

9. Perkins, Edward W.: Experimental Investigation of the Effects of Support Interference on the Drag of Bodies of Revolution at a Mach Number of 1.5. NACA RM A8B05, 1948.

[redacted]

TABLE I

FUSELAGE COORDINATES

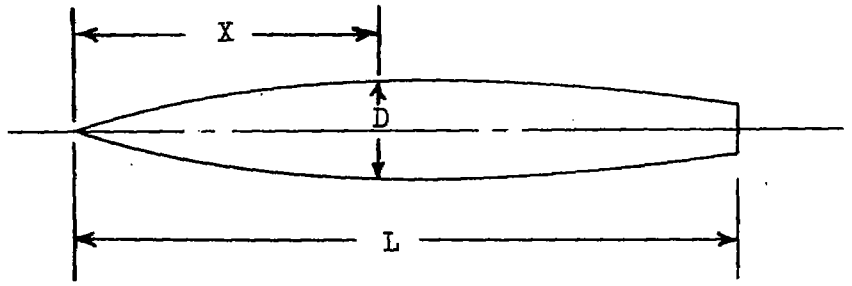

Station X/L	Diameter D/L		
	Models A, B	Model C	Model D
0	0	0	0
.1	.0246	.0245	.0417
.2	.0447	.0448	.0667
.3	.0605	.0608	.0832
.4	.0719	.0723	.0927
.5	.0793	.0800	.0981
.6	.0819	.0832	.1000
.7	.0803	.0821	.0975
.8	.0744	.0767	.0888
.9	.0642	.0669	.0795
1.0	.0497	.0533	.0700

NACA

TABLE II

Model	Sustainer Motor				Booster motor	Reference
	Type	Nozzle half angle (deg)	Specific heat ratio of exhaust gas (γ)	Average thrust loading ratio $\left(\frac{F}{A_e}\right)_{average}$, lbs/sq in.		
A-1, A-2	Modified 3.25 Mk. 7	9	1.219	260	6.25-inch ABL Deacon	3
A-3	Modified 3.25 Mk. 7	30	1.219	245	6.25-inch ABL Deacon	3
B	6.25-inch ABL Deacon	30	1.26	195	None	3
C	Modified 2.25 Mk. 11	10	1.219	140	5-inch HVAR lightweight	-
D	Standard 3.25 Mk. 7	9	1.219	260	5-inch HVAR lightweight	4

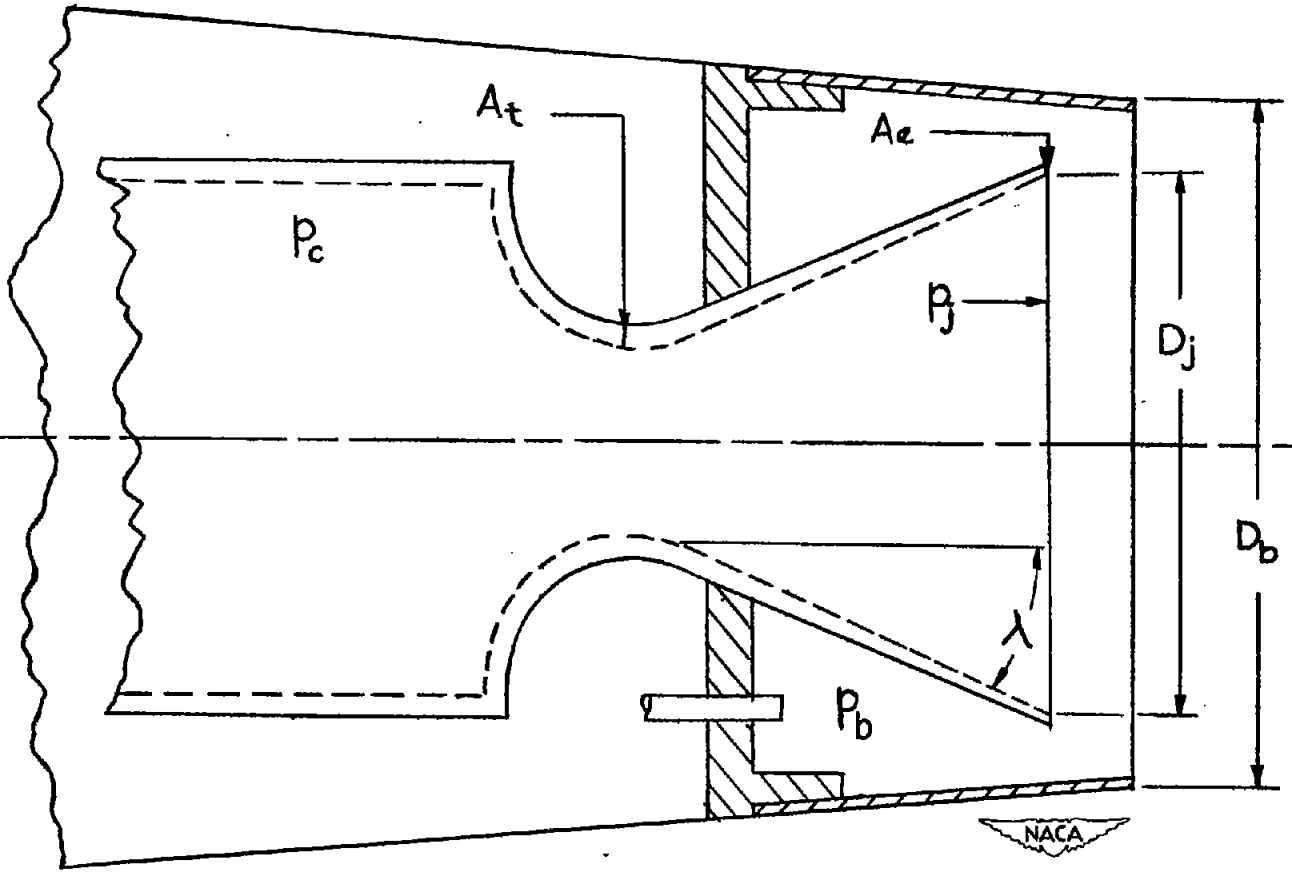

Figure 1.- General arrangement of rocket nozzle and model base.

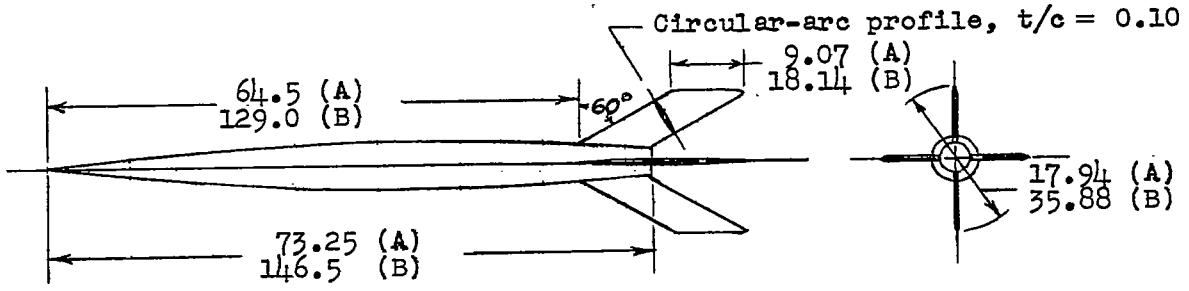

Models A and B.

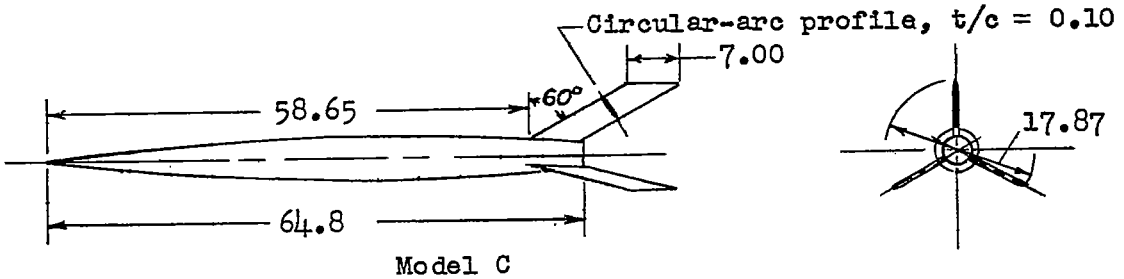

Model C

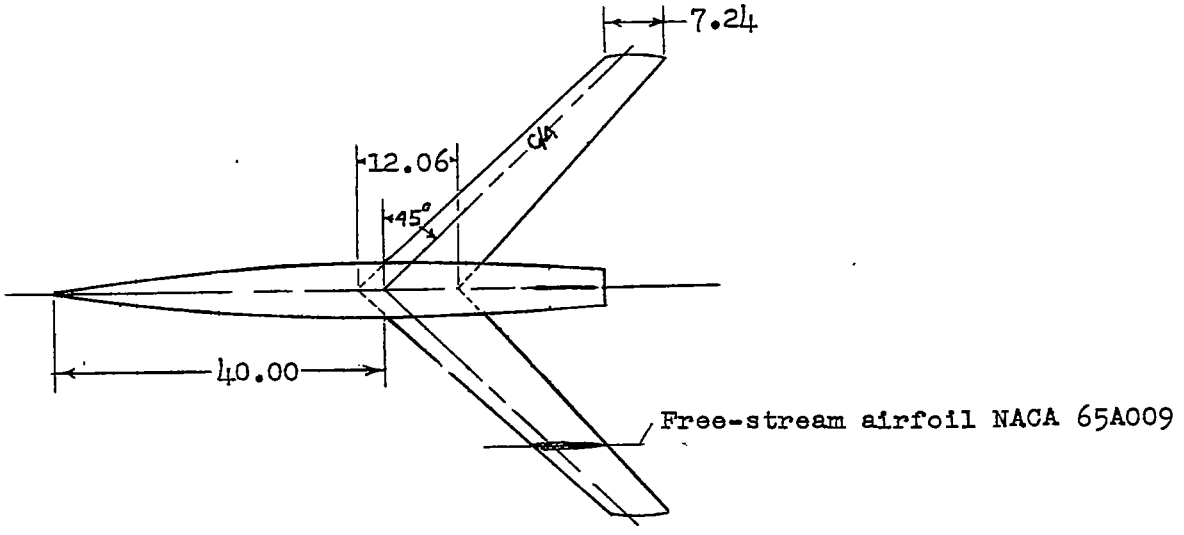

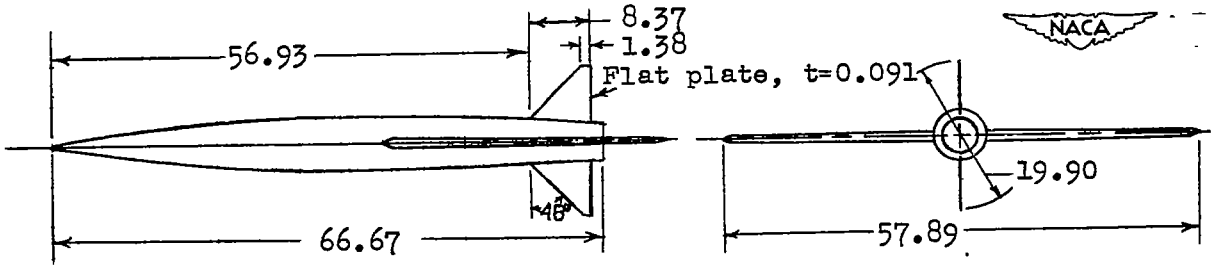

Model D

Figure 2.- External configurations of models. (Dimensions are in inches.)

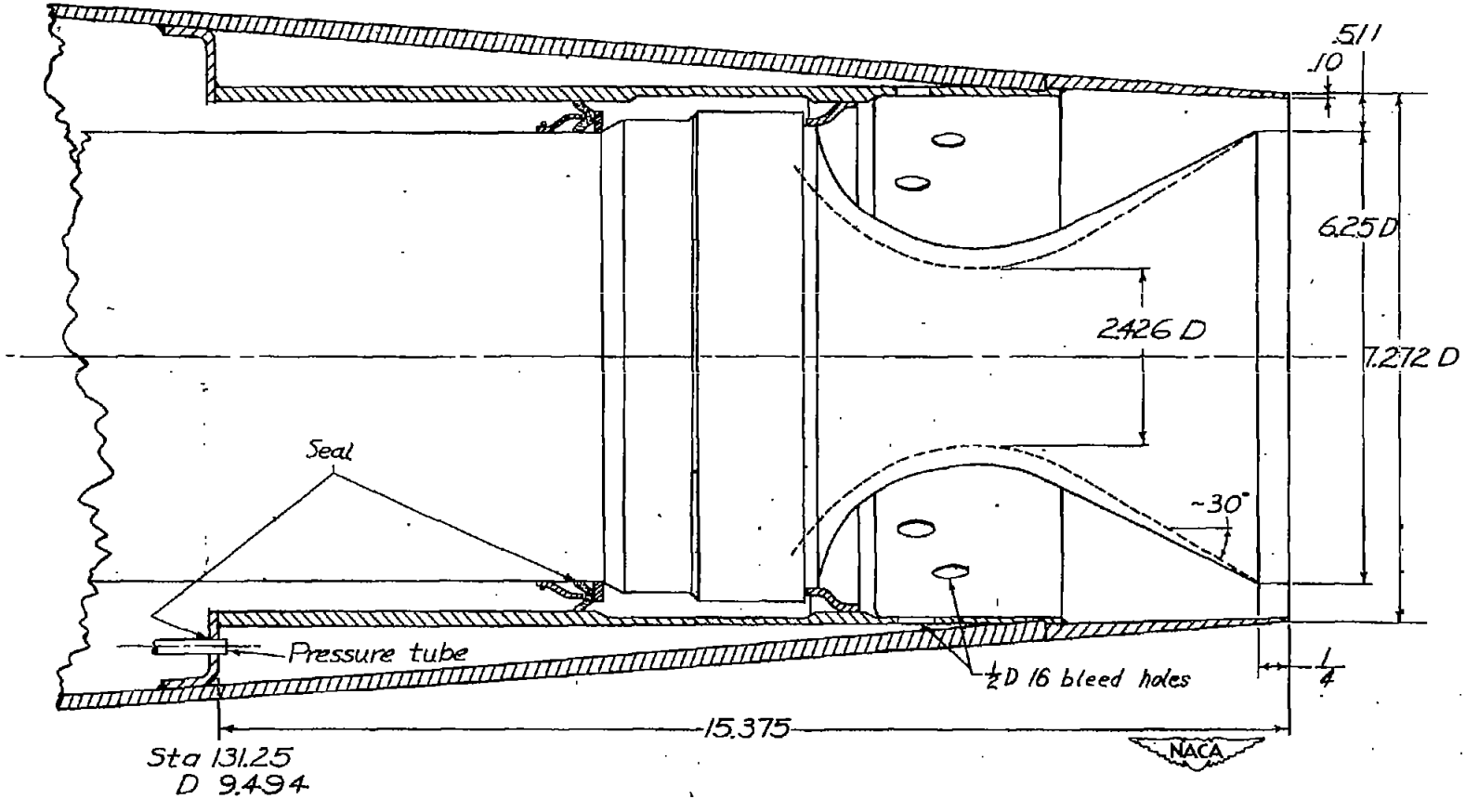

(b) Model B.

Figure 3.- Continued. (Dimensions are in inches.)

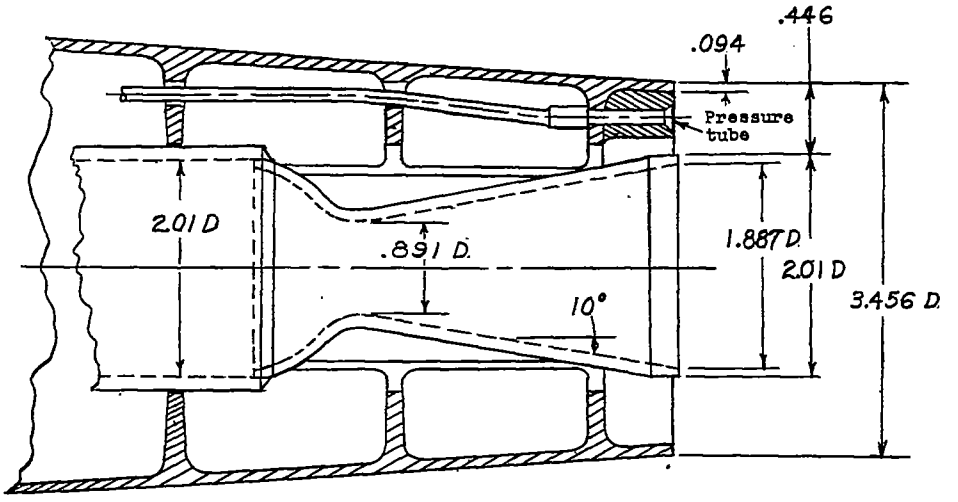

(c) Model C.

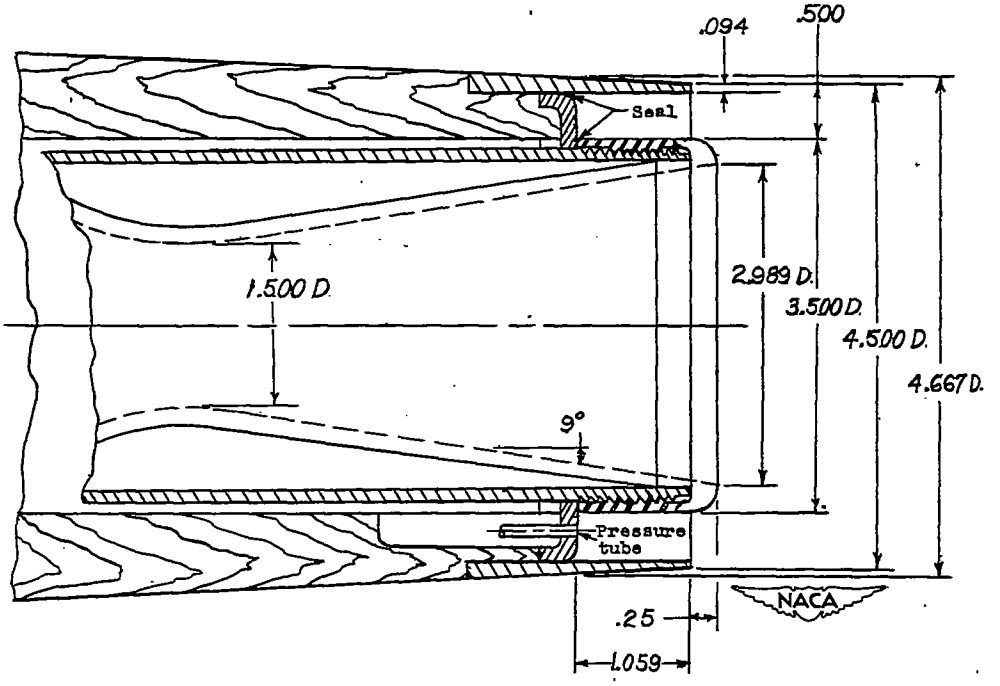

(d) Model D.

Figure 3.- Concluded. (Dimensions are in inches.)

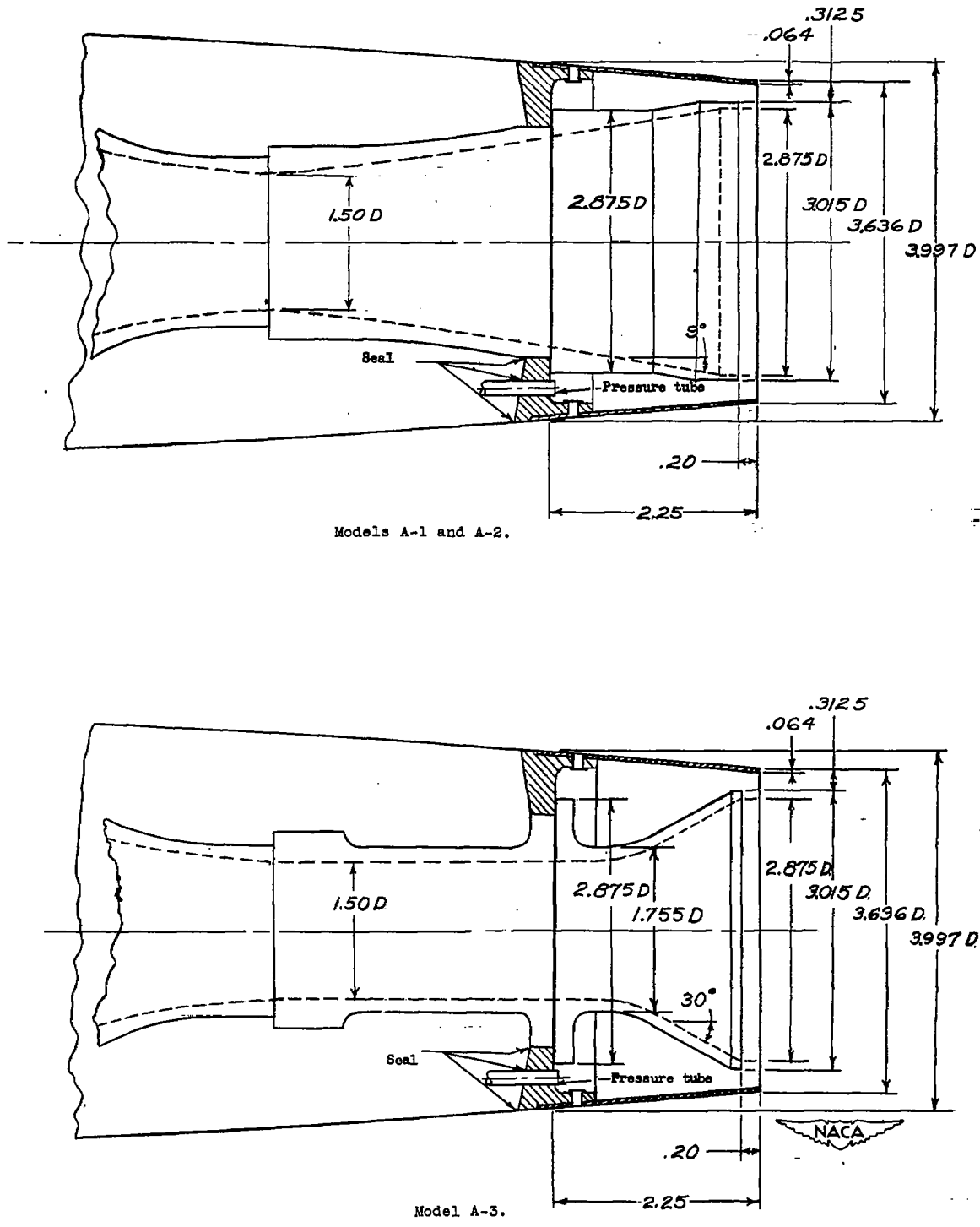

(a) Model A.

Figure 3.- Base configurations of models. (Dimensions are in inches.)

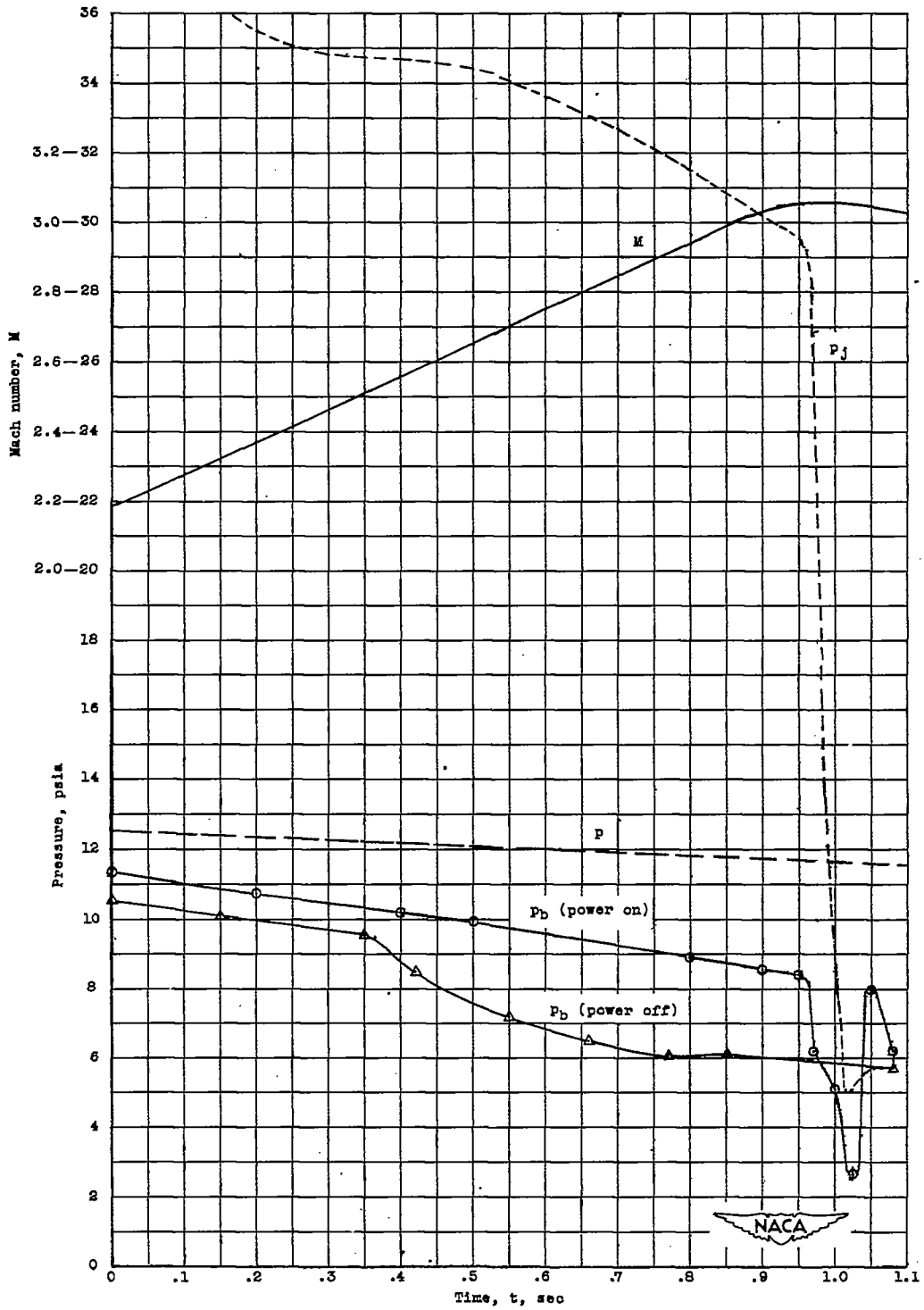

(a) Model A-1, 9° nozzle.

Figure 4.- Base-pressure data for Model A.

[redacted]

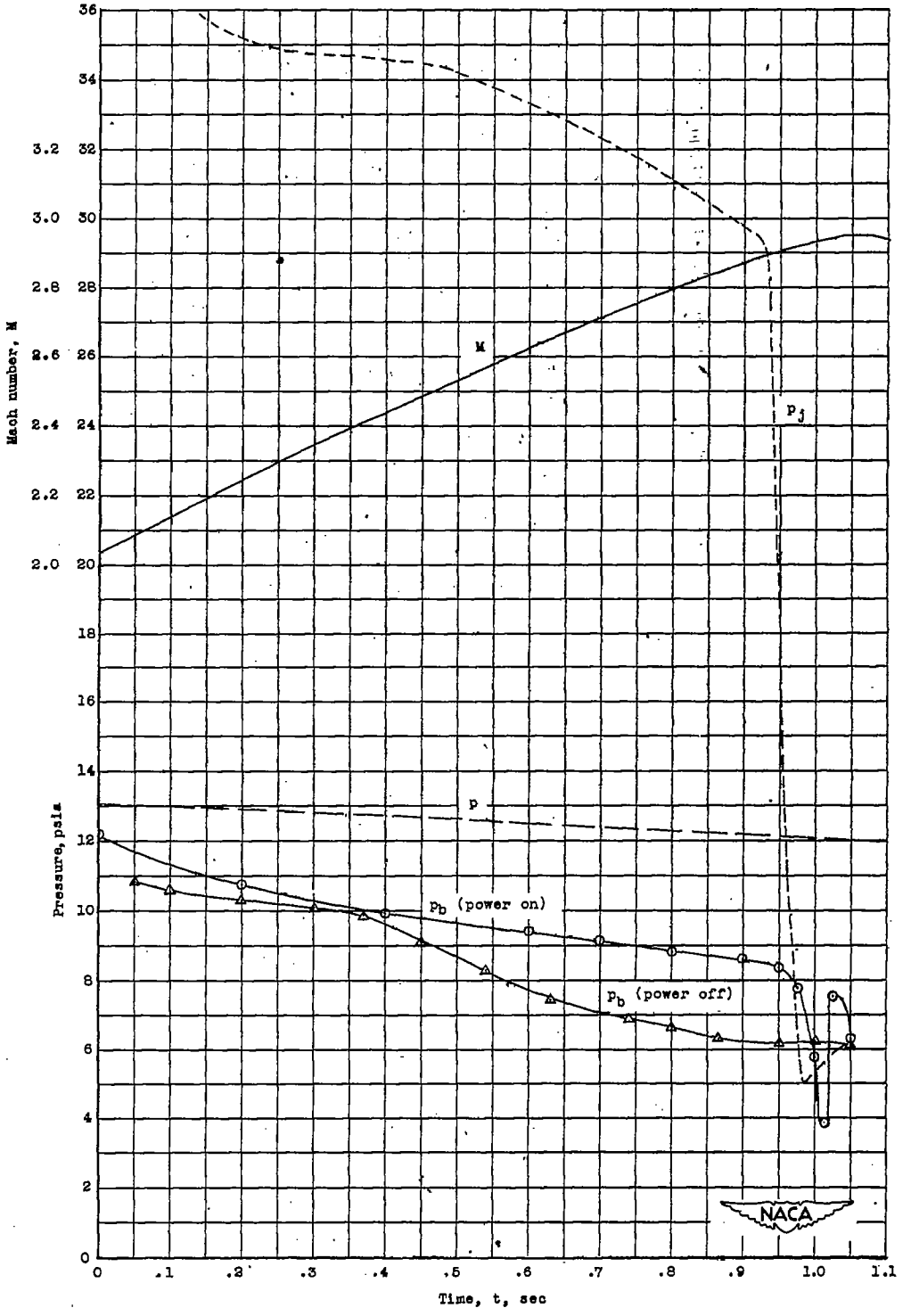

(b) Model A-2, 9° nozzle.

Figure 4.- Continued.

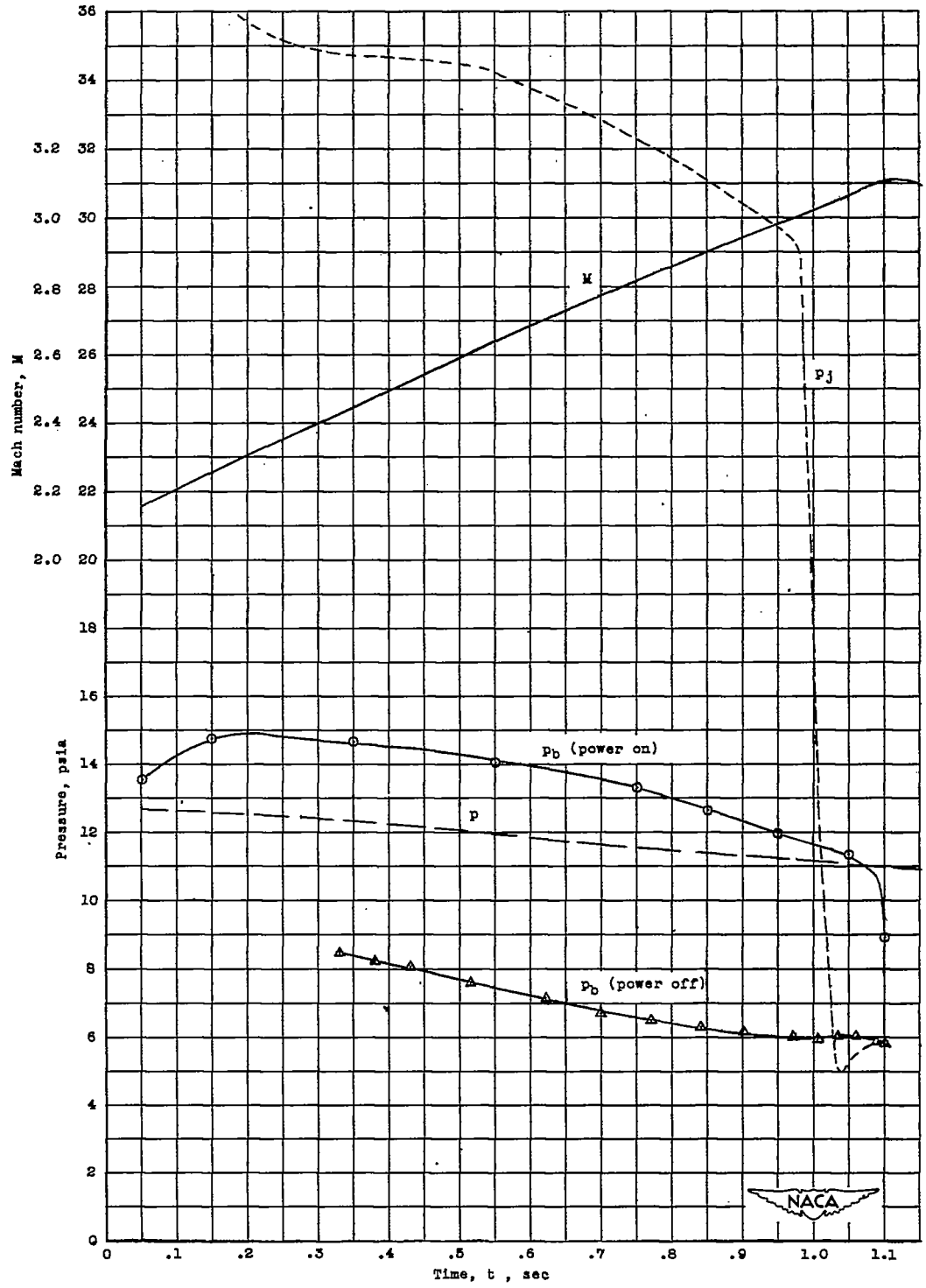

(c) Model A-3, 30° nozzle.

Figure 4.- Concluded.

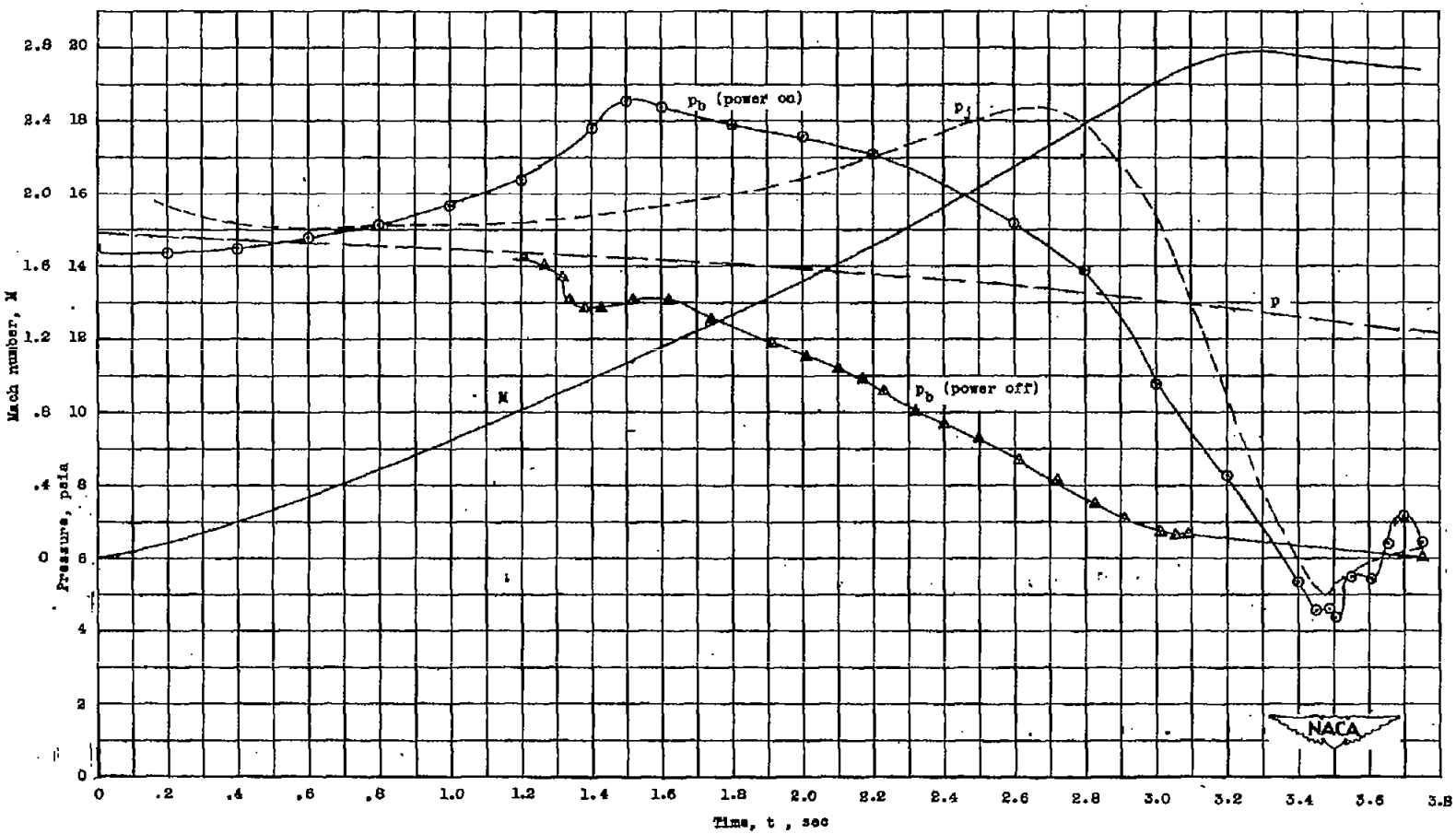

Figure 5.- Base-pressure data for Model B.

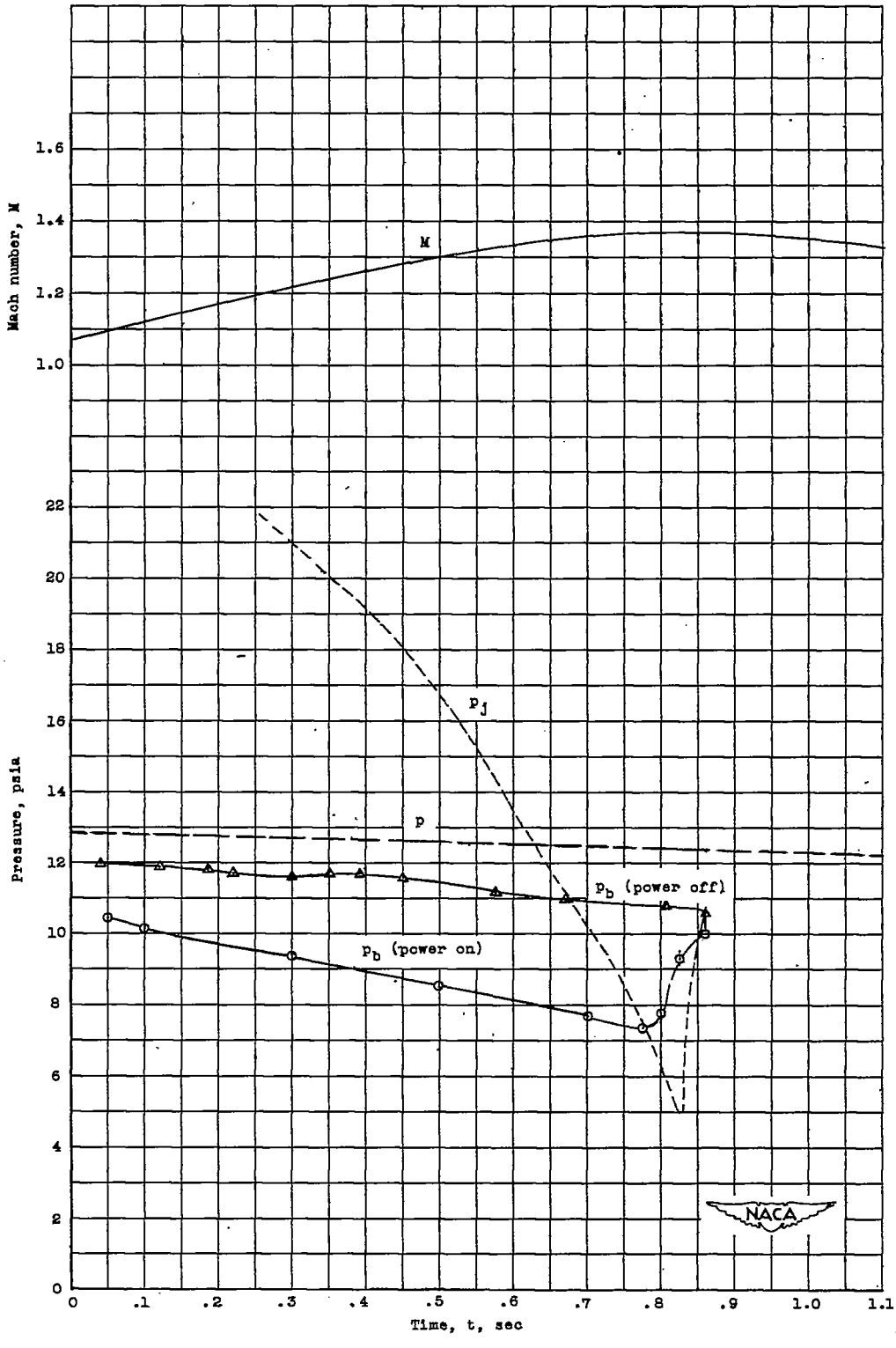

Figure 6.- Base-pressure data for Model C.

[redacted]

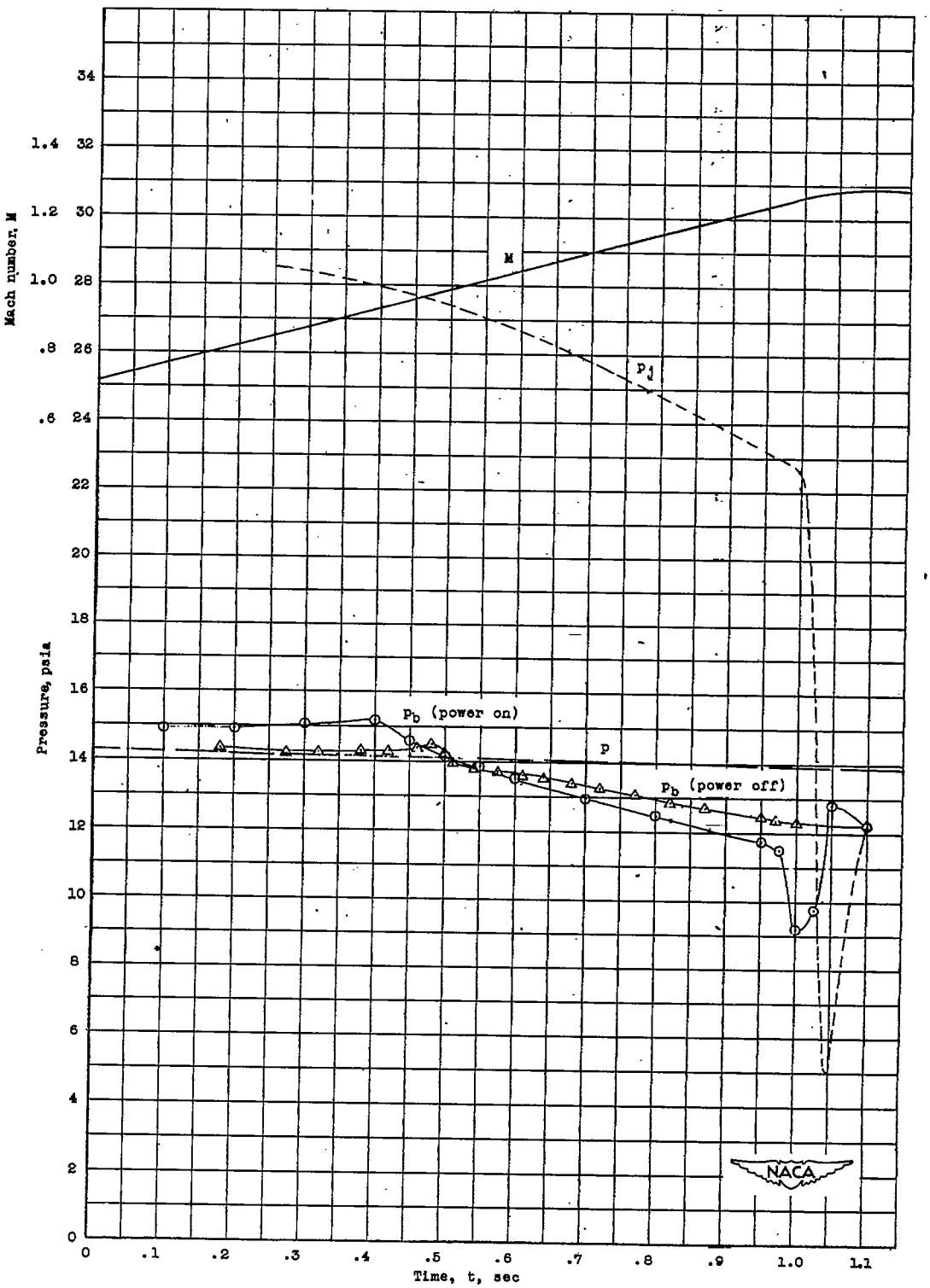

Figure 7.- Base-pressure data for Model D.

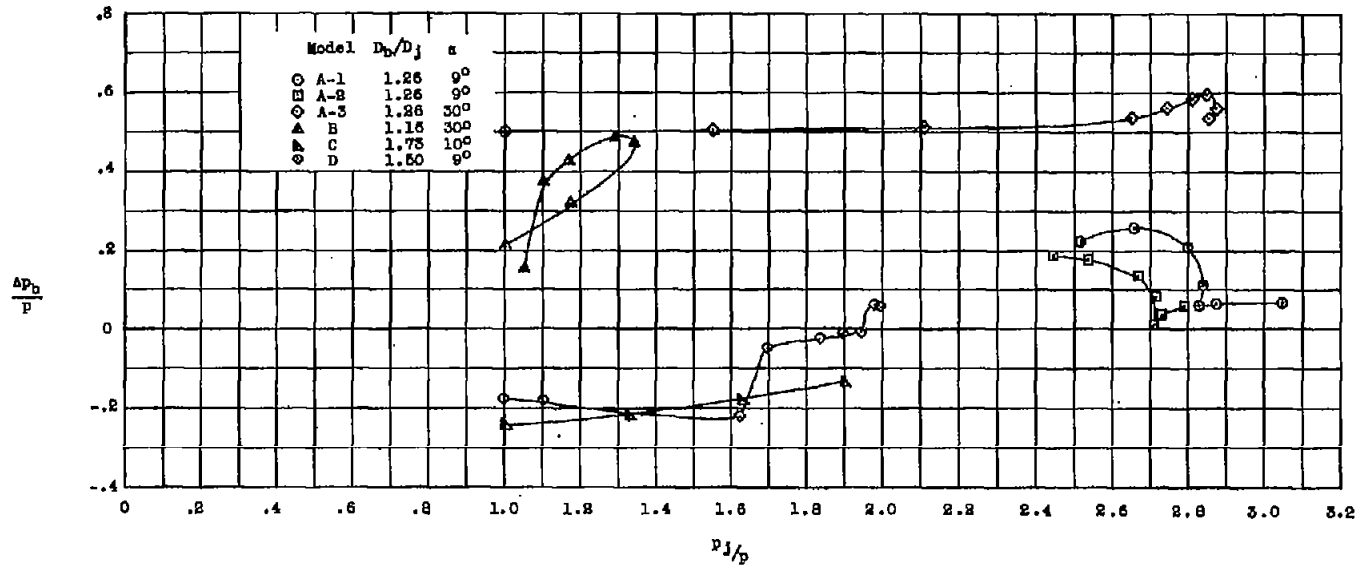

(a) Referenced to atmospheric static pressure.

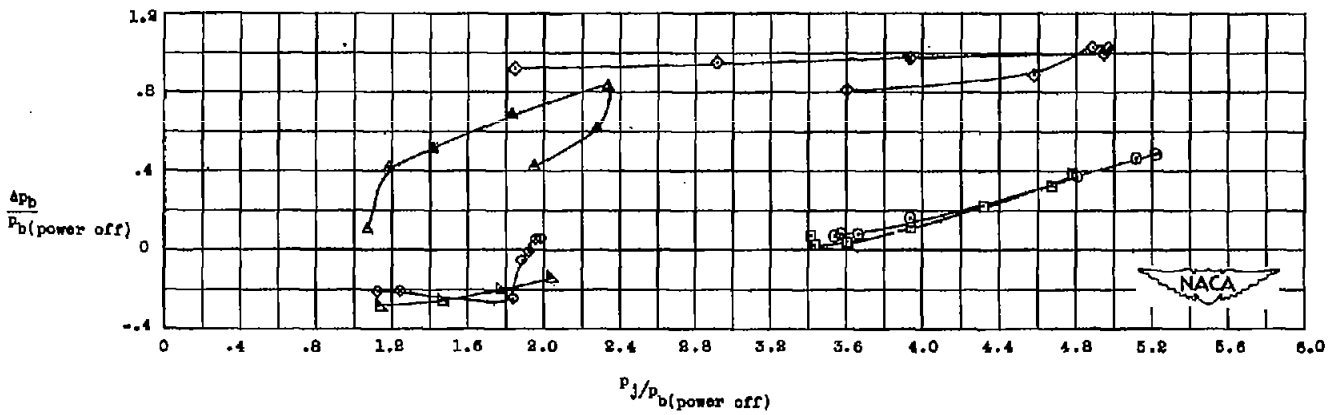

(b) Referenced to power-off base pressure.

Figure 8.- Summary of base-pressure data.

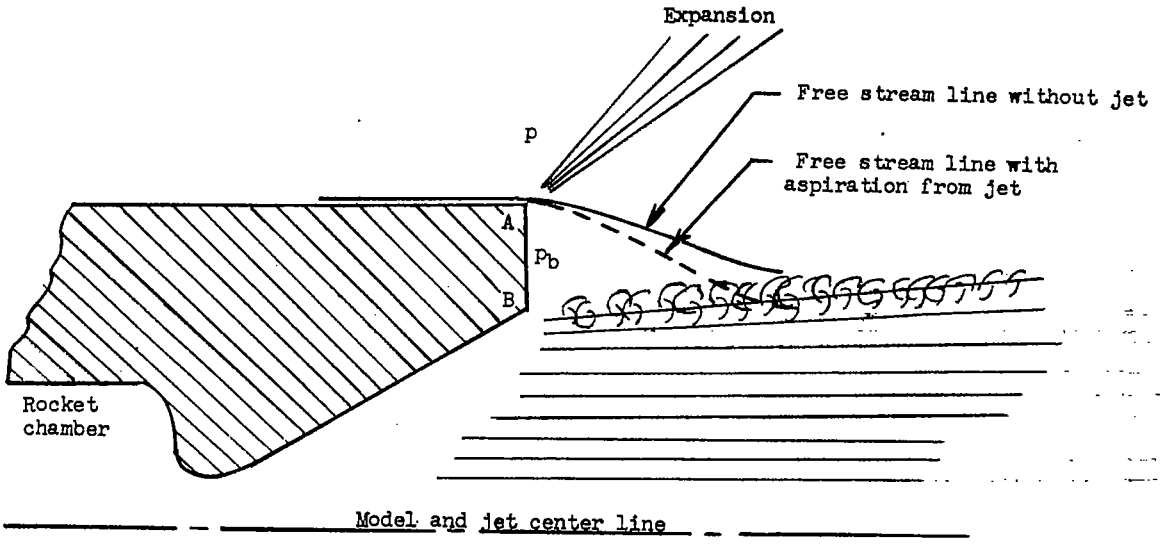

(a) General jet (viscous forces and blocking).

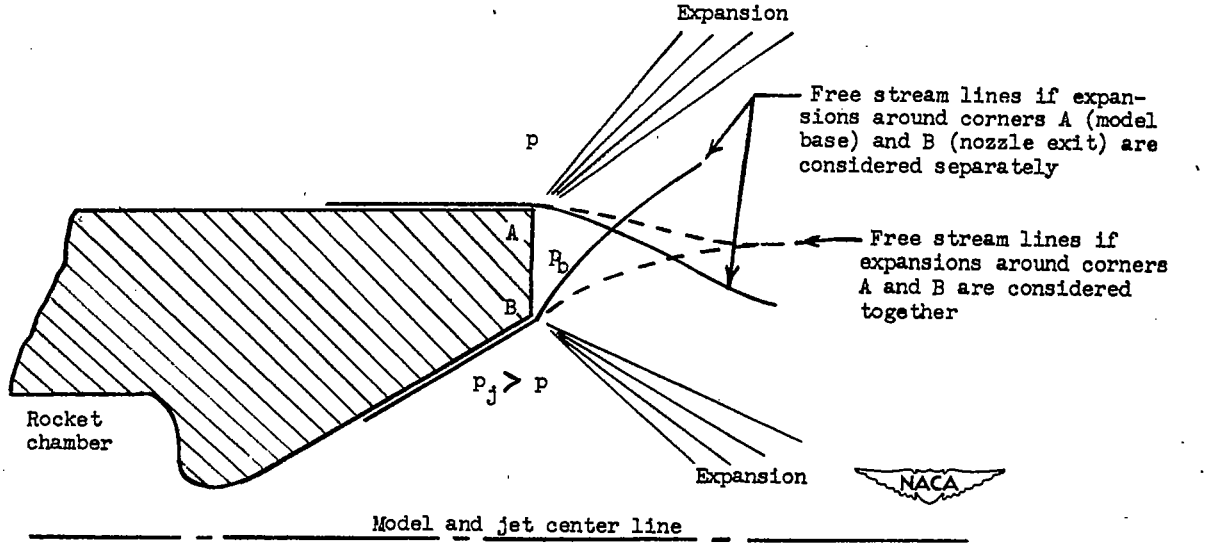

(b) Underexpanded jet (inertia forces).

Figure 9.- Schematic diagram of flow around model base and nozzle exit.

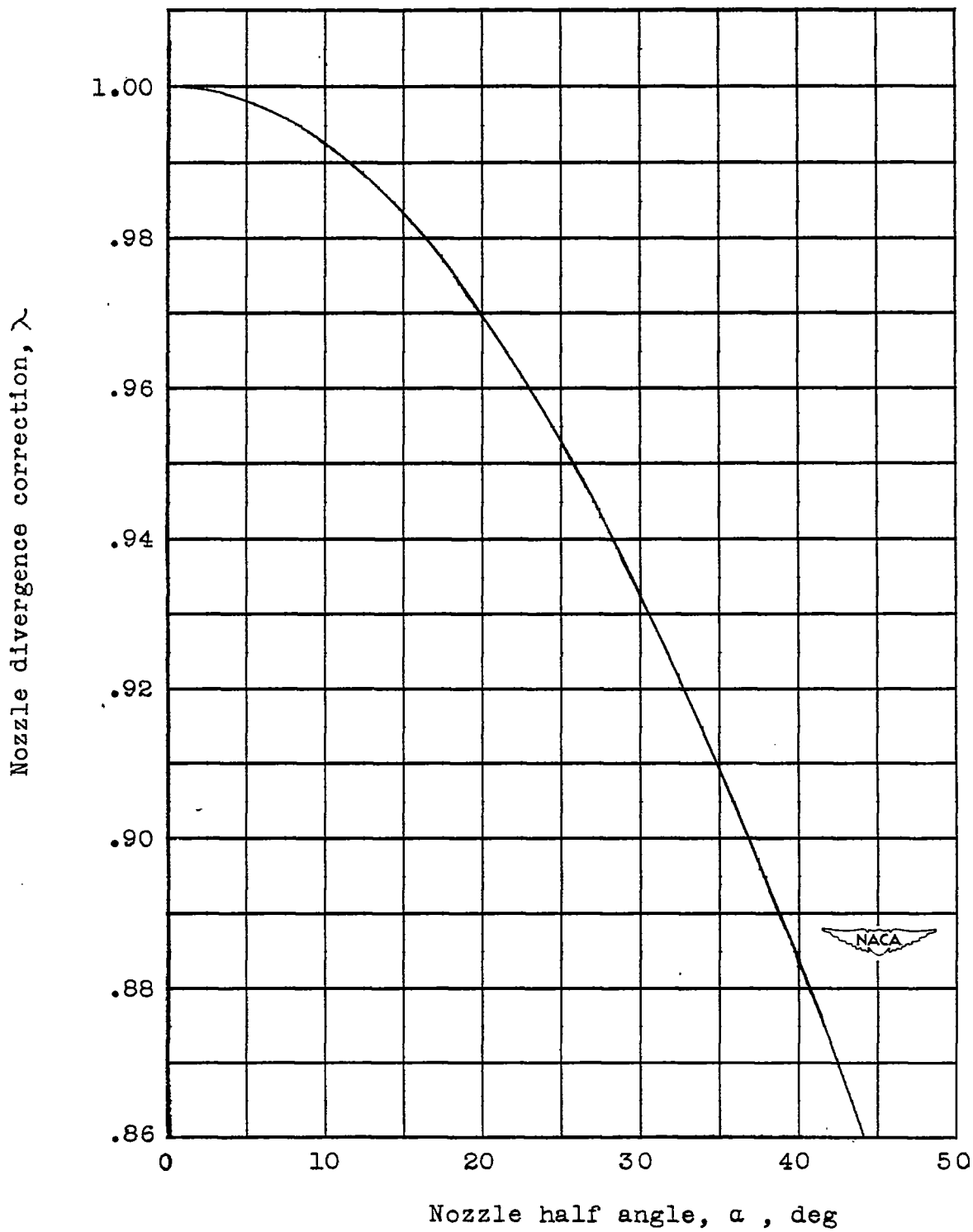

Figure 10.- Nozzle divergence correction as a function of nozzle half angle.

[redacted]

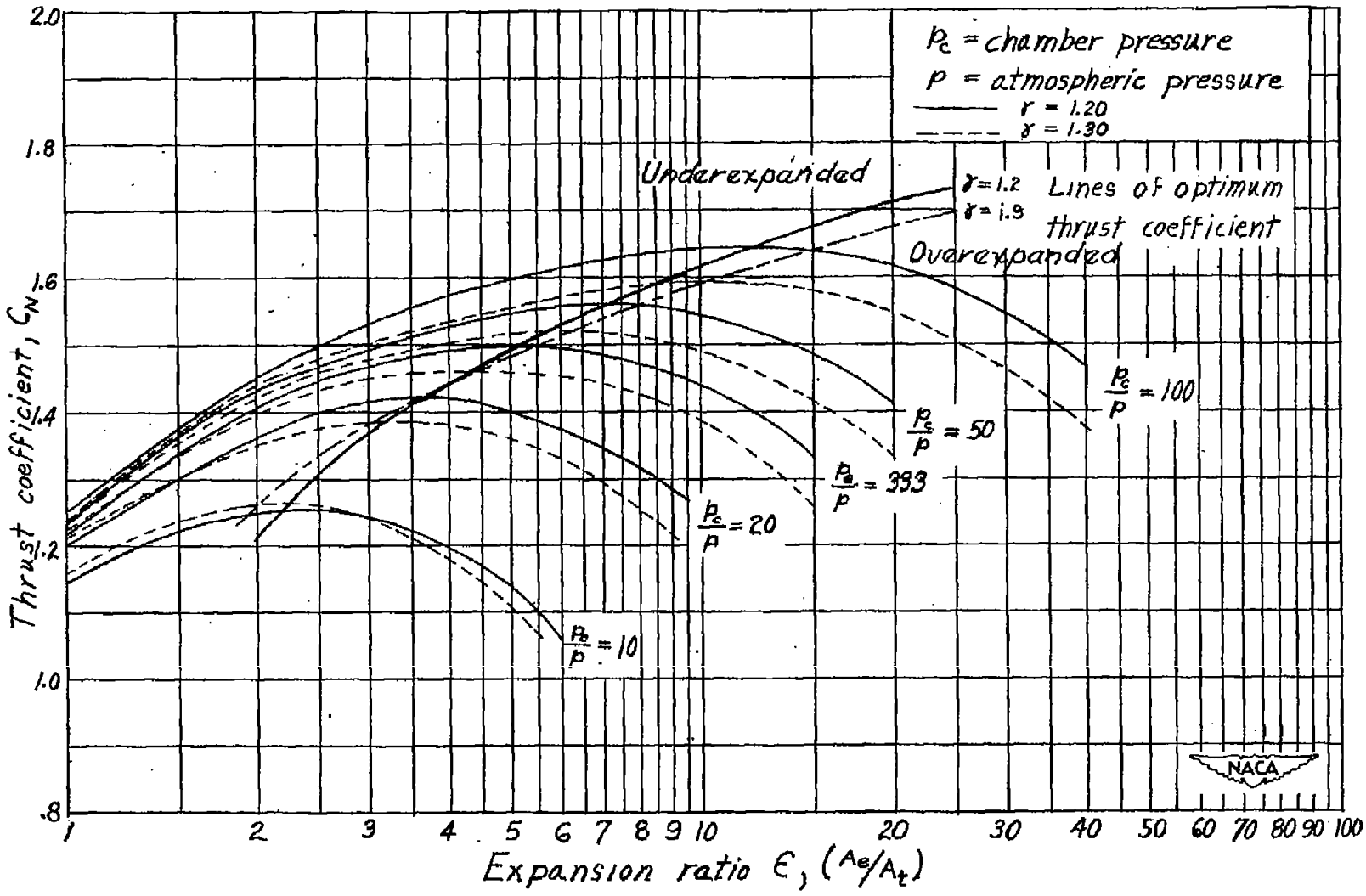

Figure 11.- Thrust coefficient as a function of area ratio and pressure ratio at $\lambda = 1.0$.